



RESEARCH LETTER

10.1002/2014GL061584

Key Points:

- Slow translation speed caused hurricane collapse
- Cold core eddy contributed to collapse
- Hurricane produced long-lived changes to upper ocean

Supporting Information:

- Readme
- Figure S1
- Figure S2
- Figure S3
- Figure S4

Correspondence to:

N. D. Walker,
nwalker@lsu.edu

Citation:

Walker, N. D., R. R. Leben, C. T. Pilley, M. Shannon, D. C. Herndon, I.-F. Pun, I.-I. Lin, and C. L. Gentemann (2014), Slow translation speed causes rapid collapse of northeast Pacific Hurricane Kenneth over cold core eddy, *Geophys. Res. Lett.*, *41*, 7595–7601, doi:10.1002/2014GL061584.

Received 22 AUG 2014

Accepted 16 OCT 2014

Accepted article online 20 OCT 2014

Published online 7 NOV 2014

Slow translation speed causes rapid collapse of northeast Pacific Hurricane Kenneth over cold core eddy

Nan D. Walker¹, Robert R. Leben², Chet T. Pilley¹, Michael Shannon², Derrick C. Herndon³, Iam-Fei Pun⁴, I.-I. Lin⁴, and Chelle L. Gentemann⁵

¹Department of Oceanography and Coastal Sciences and Coastal Studies Institute, Louisiana State University and A. & M. C., Baton Rouge, Louisiana, USA, ²Colorado Center for Astrodynamics Research, University of Colorado Boulder, Boulder, Colorado, USA, ³Cooperative Institute for Meteorological Satellite Studies, University of Wisconsin-Madison, Madison, Wisconsin, USA, ⁴Department of Atmospheric Sciences, National Taiwan University, Taipei, Taiwan, ⁵Remote Sensing Systems, Santa Rosa, California, USA

Abstract Category 4 Hurricane Kenneth (HK) experienced unpredicted rapid weakening when it stalled over a cold core eddy (CCE) on 19–20 September 2005, 2800 km SE of Hawaii. Maximum sea surface temperature (SST) cooling of 8–9°C and a minimum aeri ally averaged SST of 18.3°C (over 8750 km²) characterized its cool wake. A 3-D mixed-layer model enabled estimation of enthalpy fluxes (latent and sensible heat), as well as the relative importance of slow translation speed (U_h) compared with the preexisting CCE. As U_h dropped below 1.5 m s⁻¹, enthalpy fluxes became negative, cutting off direct ocean energy flux to HK. Although HK's weakening was attributed to wind shear, our results indicate that slow U_h and consequent intense SST cooling were the main causes. The tropical cyclone-intensified CCE experienced rapid growth in magnitude (–6 to –40 cm), increased diameter (60 to 350 km), elevated chlorophyll *a* for 4 months, and 12 month longevity.

1. Introduction

Both anticyclonic warm core eddies (WCEs) and cyclonic cold core eddies (CCEs) can rapidly impact tropical cyclone (TC) intensity changes [e.g., Emanuel, 1999; Shay et al., 2000; Lin et al., 2005, 2009a; Walker et al., 2005; Wu et al., 2007; Jaimes and Shay, 2009; Zheng et al., 2008, 2010]. Hurricanes Opal (1995), Katrina (2005), and Rita (2005) are examples of Gulf of Mexico TCs that intensified rapidly over areas of thick upper ocean warm layers [Shay et al., 2000; Jaimes and Shay, 2009]. Walker et al. [2005] demonstrated that the lowest sea surface temperatures (SSTs) (20–26°C) in Hurricane Ivan's cool wake occurred within two weak CCEs along its track. Ivan's wind speeds decreased rapidly in close proximity to these TC-intensified CCEs, demonstrating immediate negative feedback from cool waters. Measurements of Jaimes and Shay [2009] demonstrated that both Hurricanes Katrina and Rita lost strength over lowest SST regions, within TC-intensified CCEs along their tracks. Case studies in other ocean basins have supported these findings using observations and models [Emanuel, 1999; Goni and Trinanes, 2003; Halliwell et al., 2008; Zheng et al., 2008, 2010; Jaimes et al., 2011; Lin et al., 2005, 2009a, 2013].

HK formed as a tropical depression on 14 September 2005 at 118°W, 12°N in the eastern Pacific Ocean [Pasch, 2006] (Figure 1). It intensified to a category 4 hurricane by 18 September and then experienced unpredicted rapid weakening to a tropical storm in 30 h. This study investigates the evolution of oceanic and atmospheric changes along HK's track and investigates the relative importance of U_h and the weak CCE on SST cooling, as well as enthalpy fluxes, during its collapsing phase. Although a short-lived hurricane, HK caused abnormally strong and long-lived physical and biological changes to the upper ocean, which are also discussed.

2. Data and Methods

Microwave SST data were obtained as raw sensor data and as daily optimally interpolated data (MWOI) (version 4) from two sensors, the Advanced Microwave Scanning Radiometer–EOS (AMSR-E) and the Tropical Rainfall Measuring Mission's (TRMM) Microwave Imager (TMI), both with 25 × 25 km spatial resolution. These data are superior to thermal IR SST as they are not affected by clouds [Gentemann et al., 2009]. Hurricane data were obtained from the National Hurricane Center's (NHC) Tropical Cyclone Report [Pasch, 2006; Stewart, 2006] and the NOAA/Regional and Mesoscale Meteorology Branch extended best track data set (http://rammb.cira.colostate.edu/research/tropical_cyclones/tc_extended_best_track_dataset). Wind shear was calculated

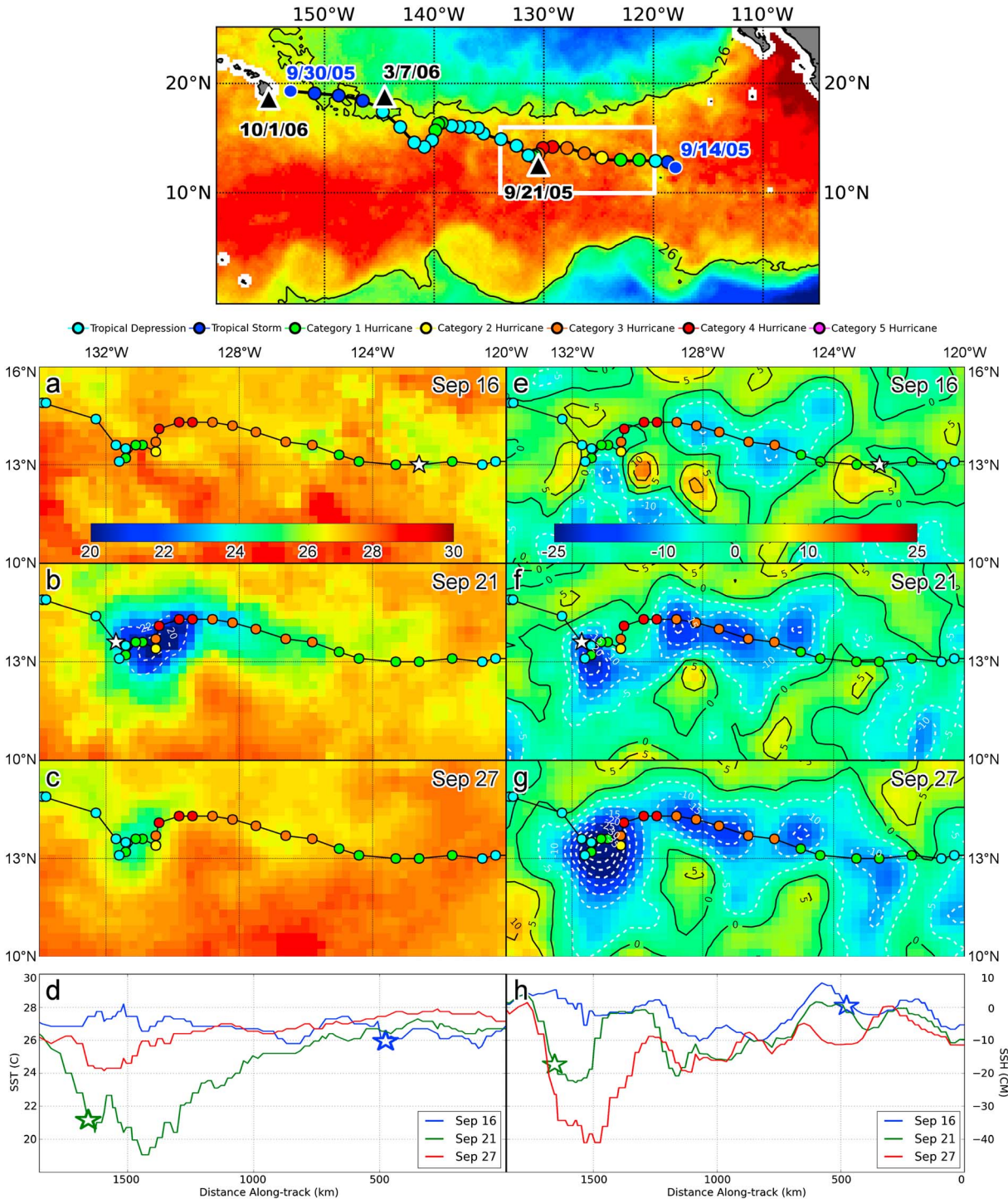


Figure 1. (top) MWOI SST ($^{\circ}\text{C}$) on 15 September 2005 and track of HK (14–30 September 2005). Intensity changes are shown with colored circles. The 26°C isotherms reveal limits to TC development. Triangles depict CCE locations: 21 September 2005 to 1 October 2006. The white box depicts the area shown in lower panels. Satellite (left) SST ($^{\circ}\text{C}$) and (right) SSHA (cm) data from (a, e) 16, (b, f) 21, and (c, g) 27 September. HK's 6 h positions and intensity are shown by colored circles. (d, h) SST and SSHA data were extracted along the track. Stars depict HK's position on 16 and 21 September. In Figures 1e–1g, positive (negative) SSHA contours are shown (5 cm increments) with solid black (dashed white) lines. In Figure 1b SST of 20°C and 22°C are superimposed to highlight the extreme cooling where HK experienced rapid weakening.

using atmospheric motion vectors [Velden *et al.*, 1997] provided by CIMSS. Mesoscale ocean eddies were tracked using daily updated and gridded sea surface height anomaly (SSHA) data (from GFO, Jason, and Envisat) produced by Colorado Center for Astrodynamic Research [Leben *et al.*, 2002] and Archiving, Validation, and Interpretation of Satellite Oceanographic data (AVISO). Sea-viewing Wide Field-of-view Sensor data were processed using the OC4 algorithm to quantify chlorophyll *a* (Chla) concentrations [O'Reilly *et al.*, 1998]. Since there were no Argo floats [Gould, 2005] within the CCE of interest, a synthetic profile was constructed using SSHA data as input to a two-layer reduced gravity scheme to derive subsurface thermal structure [Shay *et al.*, 2000; Pun *et al.*, 2007; Shay and Brewster, 2010] (Figure S1 in the supporting information). Climatological temperature profiles were obtained from the World Ocean Data Atlas 2001 (WOA01) (http://www.node.noaa.gov/OC5/OA01/pr_woa01.html) [Stephens *et al.*, 2002]. Enthalpy flux (i.e., latent and sensible heat) was computed using the bulk aerodynamic formulas [Cione and Uhlhorn, 2003; Jacob and Shay, 2003; Lin *et al.*, 2009b, 2013] based on model-simulated SST from a 3-D Price-Weller-Pinkel (3DPWP) mixed-layer model [Price *et al.*, 1994; Lin *et al.*, 2013]. For these calculations, air (T_a) and dew point temperature (T_d) data were obtained from the European Centre for Medium-Range Weather Forecasts (ECMWF) interim 6 h reanalysis and high wind speed drag coefficients were based on Powell *et al.* [2003]. The model was initialized using a spatially representative value of MWOI SST (27.8°C) (Figure S2) and a synthetic profile (based on CCE SSHA of -6.4 cm) (Figure S3) from 16 September. The values were obtained at HK's closest position to the CCE (on 20 September (0000)) (see star in Figures S2 and S3). After model initialization, SST and fluxes were computed.

3. Ocean/Atmosphere Interactions and Modifications

HK was a small but intense hurricane for 4.5 days (16–20 September) with peak winds of 59 m s^{-1} (category 4) on 18 September. It formed over 28°C waters within a relatively narrow zonal band favorable for TC development (Figure 1, top). Hurricane and tropical storm wind radii were 56 and 175 km at their maxima, and the radius of maximum wind (RMW) was 29 km from 18 to 20 September. On 18 September, HK followed Hurricane Jova by 11° of longitude. These TCs grew to hurricane strength nearly simultaneously; however, Hurricane Jova reached its peak intensity (category 3) on 20 September, as HK was weakening.

SST and SSHA images are shown on 3 days (16, 21, and 27 September) to depict oceanic conditions pre- and post-HK's passage (Figures 1a–1h). On 16 September, HK moved with a U_h of $4\text{--}5 \text{ m s}^{-1}$ over a region of weak preexisting cyclonic circulation (SSHA of -5 cm) from 124 to 129°W (Figure 1e). After passage, the SSHA had decreased 5 to 10 cm (Figures 1e, 1f, and 1h) and SST had decreased 1° to 2°C (Figures 1a, 1b, and 1d). Minimum temperatures within HK's cool wake were consistently observed at pixels closest to its track. Thus, the data in Figures 1d and 1h were extracted from subtrack pixels only. The existence of large areas of preexisting negative SSHA under HK's track likely reduced the typical rightward bias of the cool wake, shifting it toward the track. On 19 September (0600), HK's upper steering winds slackened (likely due to Hurricane Jova's outflow) causing it to drift slowly southwestward over the northern margin of a weak CCE (SSHA of -5 to -8 cm) (Figures 1e and S3) where it stalled near 13.7°N , 130.4°W . Interactions between HK and the CCE were prolonged as HK remained nearly stationary (U_h of $0.5\text{--}1.5 \text{ m s}^{-1}$) from 19 (1200) through 21 (0000) September. On 21 September, the cool wake appeared large and elliptical based on the 22°C MWOI contour (Figure 1b). Comparing MWOI SST for 16 and 21 September (Figure 1d) revealed maximum cooling of 8°C and minimum SST of 19°C under HK's track. However, raw MW SST data (from AMSR-E on 21 September) showed even more extreme cooling of 9°C and minimum SST of 18.3°C over a large area (mean of 14 pixels over 8750 km^2).

The CCE under HK grew rapidly in magnitude and size by 21 September (first available SSHA data), exhibiting full development on 27 September when a minimum SSHA of -40 cm and a maximum diameter of 350 km (based on -10 cm contour) were measured (Figures 1e–1h). The lack of SSHA data updates between 21 and 27 September made it impossible to know when the CCE reached maximum intensity. Wind speed (U_{10}) decreased rapidly from 54 (category 3) to 28 m s^{-1} (tropical storm) (Figure 2a) as HK was most affected by its cool wake during the 30 h period from 19 (1200) to 20 (1800) September (Figure 1b).

4. Model Results of SST and Enthalpy Fluxes

To quantify the relative importance of slow U_h and the CCE on the direct ocean energy supply to HK, we employed the 3DPWP mixed-layer model which was specifically designed for undertaking tropical cyclone research experiments [Price *et al.*, 1994; Lin *et al.*, 2013]. Figure 2a depicts model inputs of 6 h U_{10} , U_h , T_a , and T_d .

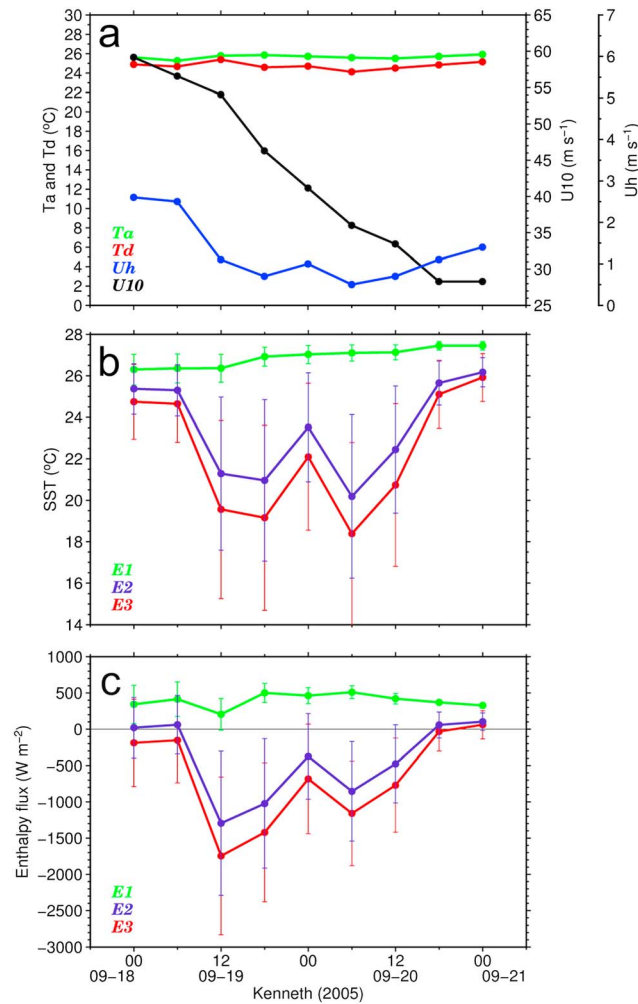


Figure 2. Data and model results during HK's rapid weakening phase. (a) Model inputs of U_{10} ($m s^{-1}$), U_h ($m s^{-1}$), T_a , and T_d . (b) SST ($^{\circ}C$) simulations for three experiments described in the text; E1 (green line), E2 (purple line), and E3 (red line) and standard deviations. (c) Enthalpy flux estimates ($W m^{-2}$) and standard deviations for E1, E2, and E3. Positive (negative) values indicate flux from ocean to atmosphere (atmosphere to ocean). Large SST variability and resultant fluxes are mainly attributed to HK tracking over the northern margin of the CCE (see Figures 1e, 1f, and S3).

Figure 2b shows the SST simulations during HK's decay phase from 19 (0000) to 21 (0000) September. The average SST within an area defined by 2.5 times the RMW (71 km) was used for the flux calculations, as TCs obtain most of their direct flux of ocean energy from this area [Cione and Uhlhorn, 2003]. Using the satellite-derived CCE profile and the observed U_h , cooling was rapid and extreme with a minimum of $18.5^{\circ}C$ on 20 September (red curve in Figure 2b). This SST is consistent with minimum observed AMSR-E SST observations of $18.3^{\circ}C$ over $>8000 km^2$. The extreme cooling is attributable to the abnormally slow U_h ($<1.5 m s^{-1}$) and uplifted thermocline within the CCE. To investigate the relative contributions of the slow U_h and CCE we ran three experiments. E1 used the climatological ocean temperature profile (rather than the SSHA-derived profile) and a more typical U_h of $5 m s^{-1}$ as input (green lines in Figures 2b and 2c). E2 used the climatological temperature profile and observed U_h (without the CCE) (purple lines). E3 used the simulated CCE profile and actual U_h (red lines). E1 revealed little surface cooling and small positive enthalpy fluxes (200 to $500 W m^{-2}$, flux from ocean to atmosphere). In E2, SST cooling was extreme and enthalpy fluxes were reversed (-500 to $-1000 W m^{-2}$, flux from atmosphere to ocean). Thus, with the low U_h (even without preexisting CCE conditions), HK received no direct energy flux from the ocean. In E3, using the CCE profile and the actual U_h , SST cooling was maximized and enthalpy

fluxes were more extreme (-1000 to $-1500 W m^{-2}$). The E1-E2 difference (green to purple line) provides a metric for the U_h effect, whereas the E2-E3 difference (purple to red line) reveals the CCE effect. The ratio of these differences approximates their relative impacts. Based on this metric, as HK was weakening, U_h contributed $\sim 75\%$, whereas the weak preexisting CCE contributed $\sim 25\%$ to SST and enthalpy flux changes.

5. Longevity of TC-Induced Changes to Upper Ocean

The SST imagery of 27 September showed considerable warming of the cool wake in 6 days (Figures 1b–1d), although the CCE continued to exhibit cooler SST, relative to surrounding waters, for ~ 3 months (not shown). Price et al. [2008] found that cool wakes as revealed in SST data typically disappear within 20 days, suggesting that the HK-generated wake was relatively long lived.

HK generated an intense (-40 cm) CCE that persisted for 12 months, traveling 2500 km (Figure 1). This CCE was #72049 in the Chelton et al. [2011] database, and it exhibited the highest value of eddy amplitude (< -15 cm) and rotational speed ($>32 cm s^{-1}$) averaged over its lifetime, compared with 105 CCEs that passed through

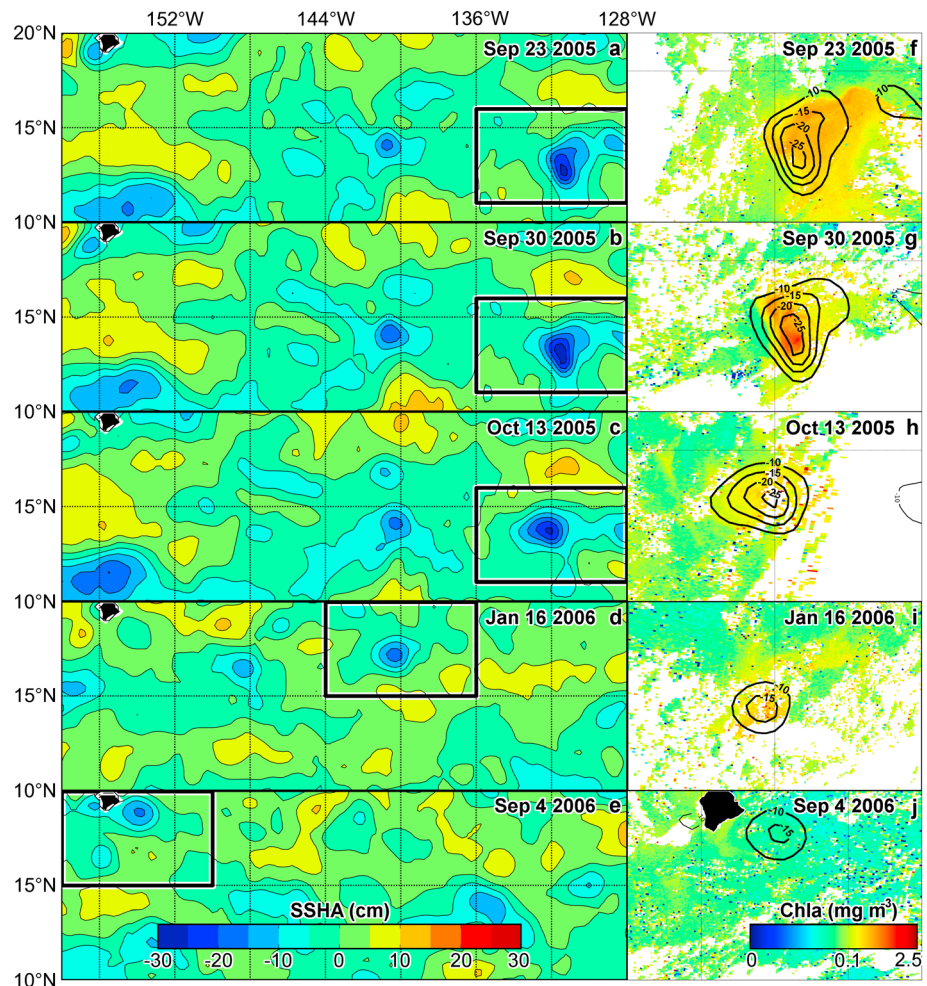


Figure 3. (left column) CCE motion toward Hawaii over ~1 year using SSHA (cm) data from 23 September, 30 September, and 13 October 2005 to 16 January and 4 September 2006. (right column) Chla (mg m^{-3}) with selected SSHA contours (-10 , -15 , -20 , and -25 cm) superimposed.

the 5° longitude area in which it formed. Its WNW track is displayed in Figure 3 using SSHA data from five selected dates between 23 September 2005 and 4 September 2006. Chla enhancement within the CCE was first clearly observed on 23 September (Figure 3f), when a mean value of 0.2 mg m^{-3} was measured over $46,000 \text{ km}^2$ (maximum was 0.35 mg m^{-3}). By 30 September, the maximum concentration increased to 1.0 mg m^{-3} suggesting that a new phytoplankton bloom had occurred due to upward injection of nutrients (Figure 3g). A similar lagged response between CCE intensification and Chla enhancement was observed after Hurricane Ivan [Walker *et al.*, 2005]. Chla concentrations decreased by the next clear view on 13 October (Figure 3h), and by 16 January 2006, the Chla area was reduced to 9200 km^2 with a maximum value of 0.25 mg m^{-3} (Figure 3i). Thereafter, cloud cover inhibited detection of Chla until 4 September 2006, when Chla values within the CCE were lower than surrounding waters south of Hawaii (Figure 3j).

6. Discussion

Regarding HK's collapse, initially, forecasters attributed HK's weakening to NNE wind shear (from Hurricane Jova's outflow) [Pasch, 2006]. However, our analysis revealed a maximum wind shear of 9.2 m s^{-1} on 19 September (Figure S4). Paterson *et al.* [2005] showed that wind shear values in this range result in weakening of 3–8 hPa, whereas HK experienced weakening of 47 hPa, suggesting that wind shear had only a minor effect on HK's weakening. Lin *et al.* [2013] observed that slow-moving TCs ($U_h < 3 \text{ m s}^{-1}$) are more impacted by oceanic factors (i.e., SST cooling and enthalpy fluxes), whereas faster-moving TCs are more impacted by

atmospheric factors (i.e., wind shear and internal dynamics). HK's rapid weakening in 30 h over its cool wake provides a clear example of how important oceanic effects can be under conditions of low U_h .

TC-forced SST cooling results mainly from vertical mixing and entrainment, transient upwelling, and heat losses (latent and sensible) to the atmosphere [Price, 1981; Shay et al., 2000]. Our model results revealed that direct oceanic heat losses did not contribute to SST cooling in this case. Price [1981] demonstrated that the contribution of transient upwelling to SST cooling increases as U_h decreases. To investigate the role of upwelling in this case, we computed isotherm upwelling ($\Delta\eta$) from the change in SSH anomaly (Δh) using the reduced gravity approximation $\Delta\eta = -g/g' \Delta h$ [Shay et al., 2000; Walker et al., 2005]. Assuming the suggested g' value 0.035 for this ocean [Shay and Brewster, 2010] and $\Delta h = -17$ cm (SSHA change from 16 to 21 September) we estimated an isotherm upwelling of 48 m. The simulated temperature profile revealed 20°C water at 48 m (Figure S1); thus, vertical mixing must have also played a role in SST cooling since upwelling alone did not explain the minimum observed cool wake SST of 18.3°C. Jaimes and Shay [2009] observed a rapid rate of upwelling (1 cm s^{-1}) when TC Rita tracked over a CCE. At this rate, the extreme cool wake from HK would have evolved in less than 2 h, helping to explain HK's rapid collapse. Regarding mixing, Jaimes et al. [2011] found that near-inertial TC energy is trapped above the thermocline within CCEs, leading to enhanced mixing at the base of the mixed layer, and subsequent strong surface cooling. In contrast, within WCEs, they found that the TC energy was transmitted downwards into the thermocline resulting in much reduced surface cooling.

HK had profound and long-lived impacts on the upper ocean. It intensified the preexisting CCE, producing one of the most energetic and long-lived cyclonic eddies in this ocean region over 16 years [Chelton et al., 2011]. Previous research has shown that TC-induced upwelling and mixing of nutrient-rich water from the upper thermocline can lead to an enhancement of Chla [Lin et al., 2003; Babin et al., 2004], especially within CCEs [e.g., Walker et al., 2005; Zheng et al., 2008]. In a study of 13 TC-induced phytoplankton blooms, Babin et al. [2004] found that Chla values returned to prestorm levels within 2 to 3 weeks. Thus, HK produced an abnormally large CCE with a long-lived Chla response that may warrant further research.

Acknowledgments

We would like to thank Jim Price and an anonymous reviewer for their comments that helped us greatly improve this paper. Robert Leben acknowledges the support from NASA Ocean Surface Topography Mission Science Team grants NNX08AR60G and NNX13AH05G. Atmospheric air and dew point temperature data are available at ECMWF. Data set: ERA Interim. URL: http://apps.ecmwf.int/datasets/data/interim_full_daily/. SSH data used in the study are available from <http://ccar.colorado.edu> and also from AVISO. Data sets: DT MSLA, URL: <http://www.avisio.altimetry.fr/index.php?id=1272>. The microwave OI SST data are available at RSS. Data set: Microwave OI SSTs. URL: <http://www.remss.com/measurements/sea-surface-temperature>. AMSR-E raw sensor data available at URL: ftp://ftp.remss.com/amsre/bmaps_v07/y2005/m09/. Kenneth's intensity and radii data are available at RAMMB of NOAA/NESDIS. Data set: Extended Best Track Data set. URL: http://rammb.cira.colostate.edu/research/tropical_cyclones/tc_extended_best_track_dataset/index.asp. Climatological temperature profiles were obtained from the World Ocean Data Atlas 2001 (WOA01) URL: http://www.node.noaa.gov/OC5/OA01/pr_woa01.html. NHC Tropical Cyclone Report for track and meteorological data. URL: <http://www.nhc.noaa.gov/data/tcr/index.php?season=2005&basin=epac>. Wind shear and geostationary satellite-derived winds can be accessed from URL: <http://tropic.ssec.wisc.edu/archive/>.

Meghan Cronin thanks James F. Price and one anonymous reviewer for their assistance in evaluating this paper.

7. Conclusions

Satellite measurements (SST and SSHA) were used in tandem with the 3DPWP model to better understand the unpredicted collapse of HK, a category 4 East Pacific hurricane. This case provides evidence that slow U_h ($< 1.5 \text{ m s}^{-1}$) can cause rapid weakening of a major TC. When HK stalled over a weak cyclonic eddy, U_h dropped below 1.5 m s^{-1} and extreme SST cooling rapidly resulted under HK. This SST cooling (SST $< 19^\circ\text{C}$, $\Delta\text{SST} = 8\text{--}9^\circ\text{C}$) was inferred to be a significant factor in HK's rapid weakening, given the reduced air-sea fluxes ($< -1000 \text{ W m}^{-2}$). Model results demonstrate that the low U_h played the more important oceanic role ($\sim 75\%$) in SST cooling and resultant negative air-sea fluxes. Thermal structure of the preexisting CCE played a lesser oceanic role ($\sim 25\%$). Wind shear estimates indicated that it played a more minor role in HK's weakening.

Long-lived upper ocean changes from HK included intensification of the preexisting CCE (from -10 to -40 cm), CCE diameter increase (from 60 to 350 km), and a large Chla response ($+0.2 \text{ mg m}^{-3}$ over $46,000 \text{ km}^2$) with a detectable Chla signature for 4 months. Our experience with the use of SSHA data in this study demonstrates an urgent need for more operational satellite altimeters to enable resolving the temporal details of TC-mesoscale eddy interactions in order to derive more accurate predictions of TC intensity changes.

References

- Babin, S. M., J. A. Carton, T. D. Dickey, and J. D. Wiggert (2004), Satellite evidence of hurricane-induced phytoplankton blooms in an oceanic desert, *J. Geophys. Res.*, *109*, C03043, doi:10.1029/2003JC001938.
- Chelton, D. B., M. Schlax, and R. M. Samelson (2011), Global observations of nonlinear mesoscale eddies, *Prog. Oceanogr.*, doi:10.1016/j.pocean.2011.01.002.
- Cione, J., and E. Uhlhorn (2003), Sea surface temperature variability in hurricanes: Implications with respect to intensity change, *Mon. Weather Rev.*, *131*, 1783–1796.
- Emanuel, K. A. (1999), Thermodynamic control of hurricane intensity, *Nature*, *401*, 665–669.
- Gentemann, C. L., et al. (2009), MISST The multi-sensor improved sea surface temperature project, *Oceanography*, *22*(2), 76–87.
- Goni, G. J., and J. A. Trinanes (2003), Ocean thermal structure monitoring could aid in the intensity forecast of tropical cyclones, *Eos Trans. AGU*, *84*(51), 573–578, doi:10.1029/2003EO510001.
- Gould, J. (2005), From Swallow floats to Argo: The development of neutrally buoyant floats, *Deep Sea Res., Part II*, *52*(3–4), 529–543.
- Halliwel, G. R., Jr., L. K. Shay, S. D. Jacob, O. M. Smedstad, and E. W. Uhlhorn (2008), Improving ocean model initialization for coupled tropical cyclone forecast models using GODAE nowcasts, *Mon. Weather Rev.*, *136*, 2576–2591, doi:10.1175/2007MWR2154.1.

- Jacob, S. D., and L. K. Shay (2003), The role of oceanic mesoscale features on the tropical-cyclone induced mixed layer response, *J. Phys. Oceanogr.*, *33*, 649–676.
- Jaimes, B., and L. K. Shay (2009), Mixed layer cooling in mesoscale oceanic eddies during Hurricanes Katrina and Rita, *Mon. Weather Rev.*, *137*, 4188–4207, doi:10.1175/2009MWR2849.1.
- Jaimes, B., L. K. Shay, and G. R. Halliwell (2011), The response of quasigeostrophic oceanic vortices to tropical cyclone forcing, *J. Phys. Oceanogr.*, *41*, 1965–1985, doi:10.1175/JPO-D-11-06.1).
- Leben, R. R., G. H. Born, and B. R. Engebret (2002), Operational altimeter data processing for mesoscale monitoring, *Mar. Geod.*, *25*, 3–18.
- Lin, I., W. T. Liu, C.-C. Wu, G. T. F. Wong, C. Hu, Z. Chen, W.-D. Liang, Y. Yang, and K.-K. Liu (2003), New evidence for enhanced ocean primary production triggered by tropical cyclone, *Geophys. Res. Lett.*, *30*(13), 1718, doi:10.1029/2003GL017141.
- Lin, I. I., C. C. Wu, K. Emanuel, I. H. Lee, C. R. Wu, and I. F. Pun (2005), The interaction of Super typhoon Maemi (2003) with a warm ocean eddy, *Mon. Weather Rev.*, *133*(9), 2635–2649.
- Lin, I.-I., C.-H. Chen, I.-F. Pun, W. T. Liu, and C.-C. Wu (2009a), Warm ocean anomaly, air sea fluxes, and the rapid intensification of tropical cyclone Nargis (2008), *Geophys. Res. Lett.*, *36*, L03817, doi:10.1029/2008GL035815.
- Lin, I. I., I. F. Pun, and C. C. Wu (2009b), Upper-ocean thermal structure and the western North Pacific category 5 typhoons. Part II: Dependence on translation speed, *Mon. Weather Rev.*, *137*, 3744–3757.
- Lin, I. I., P. Black, J. F. Price, C. Y. Yang, S. S. Chen, C. C. Lien, P. A. Harr, N. H. Chi, C. C. Wu, and E. A. D'Asaro (2013), An ocean coupling potential intensity index for tropical cyclones, *Geophys. Res. Lett.*, *40*, 1878–1882, doi:10.1002/grl.50091.
- O'Reilly, J. E., S. Maritorena, B. G. Mitchell, D. Siegel, K. Carder, S. Garver, M. Kahru, and C. McClain (1998), Ocean color chlorophyll algorithms for SeaWiFS, *J. Geophys. Res.*, *103*, 24,937–24,953.
- Pasch, R. J. (2006), Tropical Cyclone Report—Hurricane Kenneth, National Hurricane Center. [Available at <http://www.nhc.noaa.gov/>]
- Paterson, L., B. Hanstrum, N. Davidson, and J. Weber (2005), Influence of environmental vertical wind shear on the intensity of hurricane-strength tropical cyclones in the Australian region, *Mon. Weather Rev.*, *133*, 3644–3660.
- Powell, M. D., P. J. Vickery, and T. A. Reinhold (2003), Reduced drag coefficient for high wind speeds in tropical cyclones, *Nature*, *422*, 279–283.
- Price, J. F. (1981), Upper ocean response to a hurricane, *J. Phys. Oceanogr.*, *11*, 153–175.
- Price, J. F., T. B. Sanford, and G. Z. Forristall (1994), Forced stage response to a moving hurricane, *J. Phys. Oceanogr.*, *24*, 233–260.
- Price, J. F., J. Morzel, and P. P. Niiler (2008), Warming of SST in the cool wake of a moving hurricane, *J. Geophys. Res.*, *113*, C07010, doi:10.1029/2007JC004393.
- Pun, I. F., I. I. Lin, C. R. Wu, D. H. Ko, and W. T. Liu (2007), Validation and application of altimetry-derived upper ocean thermal structure in the western North Pacific Ocean for typhoon-intensity forecast, *IEEE Trans. Geosci. Rem. Sens.*, *45*, 1616–1630.
- Shay, L. K., and J. K. Brewster (2010), Oceanic heat content variability in the Eastern Pacific Ocean for hurricane intensity forecasting, *Mon. Weather Rev.*, *138*, doi:10.1175/2010MWR3189.1.
- Shay, L. K., G. J. Goni, and P. G. Black (2000), Effects of a warm oceanic feature on Hurricane Opal, *Mon. Weather Rev.*, *128*, 1366–1383.
- Stephens, C., J. I. Antonov, T. P. Boyer, M. E. Conkright, R. A. Locarnini, T. D. O'Brien, and H. E. Garcia (2002), World Ocean Atlas 2001 Volume 1: Temperature, in *NOAA Atlas NESDIS 49*, edited by S. Levitus, U.S. Government Printing Office, Washington, D. C.
- Stewart, S. R. (2006), Tropical Cyclone Report, Hurricane Jova, Nat. Hurricane Center. [Available at www.nhc.gov/]
- Velden, C. S., C. Hayden, S. Nieman, W. Menzel, S. Wanzong, and J. Goerss (1997), Upper-Tropospheric winds derived from geostationary satellite water vapor observations, *Bull. Am. Meteorol. Soc.*, *78*, 173–195.
- Walker, N. D., R. R. Leben, and S. Balasubramanian (2005), Hurricane-forced upwelling and chlorophyll a enhancement within cold-core cyclones in the Gulf of Mexico, *Geophys. Res. Lett.*, *32*, L18610, doi:10.1029/2005GL023716.
- Wu, C.-C., C.-Y. Lee, and I.-I. Lin (2007), The effect of the ocean eddy on tropical cyclone intensity, *J. Atmos. Sci.*, *64*, 3562–3578.
- Zheng, Z.-W., C.-R. Ho, and N.-J. Kuo (2008), Importance of pre-existing oceanic conditions to upper ocean response induced by Super Typhoon Hai-Tang, *Geophys. Res. Lett.*, *35*, L20603, doi:10.1029/2008GL035524.
- Zheng, Z.-W., C.-R. Ho, Q. Zheng, Y.-T. Lo, N.-J. Kuo, and G. Gopalakrishnan (2010), Effects of pre-existing cyclonic eddies on upper ocean response to Category 5 typhoon in the western North Pacific, *J. Geophys. Res.*, *115*, C09013, doi:10.1029/2009JC005562.